International Journal of Bioelectromagnetism
IJBEM

Volume 2, Number 2, pp. 341-351, 2000.

On the Effects of Model Errors on Forward and Inverse ECG Problems

J. Hyttinen, H.-G. Puurtinen, P. Kauppinen, J. Nousiainen, P. Laarne, and J. Malmivuo

Ragnar Granit Institute, Tampere University of Technology
P.O. Box 692, FIN-33101 Tampere, Finland

Correspondence: *jari.hyttinen@tut.fi*

Abstract. Models of the human thorax are employed for forward and inverse estimation of ECG potentials and cardiac sources, respectively. The accuracy of the simulations depends on the accuracy of the model. In order to evaluate the effect of the changes in model parameters, three accurate models of the thorax as a volume conductor were constructed and some of their parameters were varied. A model based on the Visible Human Man data and two models based on an individual MR-images gated in systole and diastole were constructed. The VHM model was employed to estimate the effects of the blood masses and the importance of the accurate tissue resistivity values on forward ECG problem. The two models based on MR-image sets were employed to assess the importance of the anatomical changes due to the mechanical function of the heart, namely the changes in major blood masses and the shape of the cardiac muscle on both forward and inverse ECG problems. The results indicated the importance of accuracy in modeling the thorax as a volume conductor, e.g. the phase of the cardiac cycle should be accounted for accurate forward or inverse solution.

Keywords: *Forward and inverse ECG problem, thorax model, Finite difference method, tissue impedance inhomogeneities*

Introduction

The shape and inhomogeneities of the human thorax as a volume conductor affect the electric field generated by the heart [1], thus the accuracy of the forward and inverse problem depends on the accuracy of the model. The well-known importance of the Brody effect of the intracardial blood masses and studies regarding the changes of ECG parameters in conditions where the tissue impedance changes [2,3] gives rise to the following questions

- What is the importance of various blood masses?
- What is the effect of changes in tissue conductivity values?
- What are the effects of the changes in blood masses due to the heartbeat?
- Should we have to use models that include the anatomical changes?

In this paper three separate studies are introduced to analyze these problems;

- Study1: Effect of the blood masses
- Study2: Effect of the changes in tissue conductivity
- Study3: Effect of the anatomical changes due to heart beat

Methods

Models developed

Three models were utilized. All developed models of the human thorax as a volume conductor were based on the finite difference method (FDM) [4]. In all cases a set of transversal thorax images were used. These images were segmented based on IARD method [5] providing the volume elements of the thorax and its inhomogeneities. Practically all structures visible in the reduced accuracy images were segmented. The segmented volume data was employed to construct an FDM model of the thorax as a volume conductor. Due to the rectangular grid of the FDM method, the segmented voxels give directly the elements for FDM model construction [4].

Model based on Visible Human Man (VHM): The anatomy of the model was derived from the US National Library of Medicine's Visible Human Man data (VHM). The original accuracy of the cryosection images of the VHM is large (1216 * 2048 pixels). For data storage and image analysis the accuracy was decreased to 250*250 pixels. The inhomogeneities modelled include lungs, heart and skeletal muscle, kidneys, liver, trachea, stomach, colon, heart and body fat, all bone structures and blood masses as indicated in Table I. The outlook of the model is presented in Figure 1.

Two models representing the changes of the anatomy due to the heart beat: The anatomy of the model was derived from a set of MR images kindly provided by Professor Robert Patterson, University of Minnesota. The image data include twelve sets of MR images showing horizontal slices of thorax gated to twelve time instances of the cardiac cycle. The slice thickness was 0.5 cm and image resolution 256*256 pixels. Two image sets presenting the anatomy during systole and diastole were segmented. The modelled inhomogeneitis include intracardiac blood masses, heart muscle, pericardial fat, and other blood masses: aorta, inferior and superior vena cava, pulmonary arteries and veins, carotid arteries, jugular veins and some minor visible vessels. Other segmented tissues include skeletal muscle, body fat, lungs, kidneys, liver, trachea, stomach, and all bone structures. An example of the diastolic and systolic MR images with their segmented equivalents is shown in Fig. 2. The volumes of different inhomogeneities are shown in Table 2.

TABLE 1. *The resistivity values used in the models [6,7].*

Organ/tissue	Resistivity
skeletal muscle	400
fat	2000
bone	2000
skull	17760
gray matter, white matter	222
stomach	400
liver	600
left lung, right lung	1325
heart muscle	450
heart fat	2000
blood masses	150

classified blood masses include: left atrium, right atrium, left ventricle, right ventricle, aortic arch, ascending aorta, descending aorta, superior vena cava, inferior vena cava, carotid artery, jugular vein, pulmonary artery, pulmonary vein, other blood	
other tissues and organs	460

TABLE 2. *The volumes of different tissues and their relative difference in end diastole and end systole models.*

Tissue	Volume [L] **Diastole**	Volume [L] **Systole**	**Relative Difference**
Heart Muscle	0.29	0.28	-2.2%
Heart Fat	0.12	0.14	10.8%
Left Atrium	0.03	0.05	56.7%
Right Atrium	0.05	0.08	51.2%
Left Ventricle	0.09	0.05	-44.2%
Right Ventricle	0.15	0.06	-57.9%
Aortic Arch	0.02	0.03	35.0%
Ascending Aorta	0.03	0.04	14.5%
Carotid Artery	0.01	0.01	6.6%
Descending Aorta	0.06	0.07	15.5%
Inferior Vena Cava	0.03	0.03	4.7%
Jugular Vein	0.02	0.03	48.1%
Pulmonary Artery	0.08	0.15	79.4%
Pulmonary Vein	0.03	0.02	-48.6%
Superior Vena Cava	0.02	0.02	-3.7%
Other Blood	0.03	0.05	63.5%
Other Tissues	18.80	18.78	-0.1%
Totals	19.88	19.88	0.0%

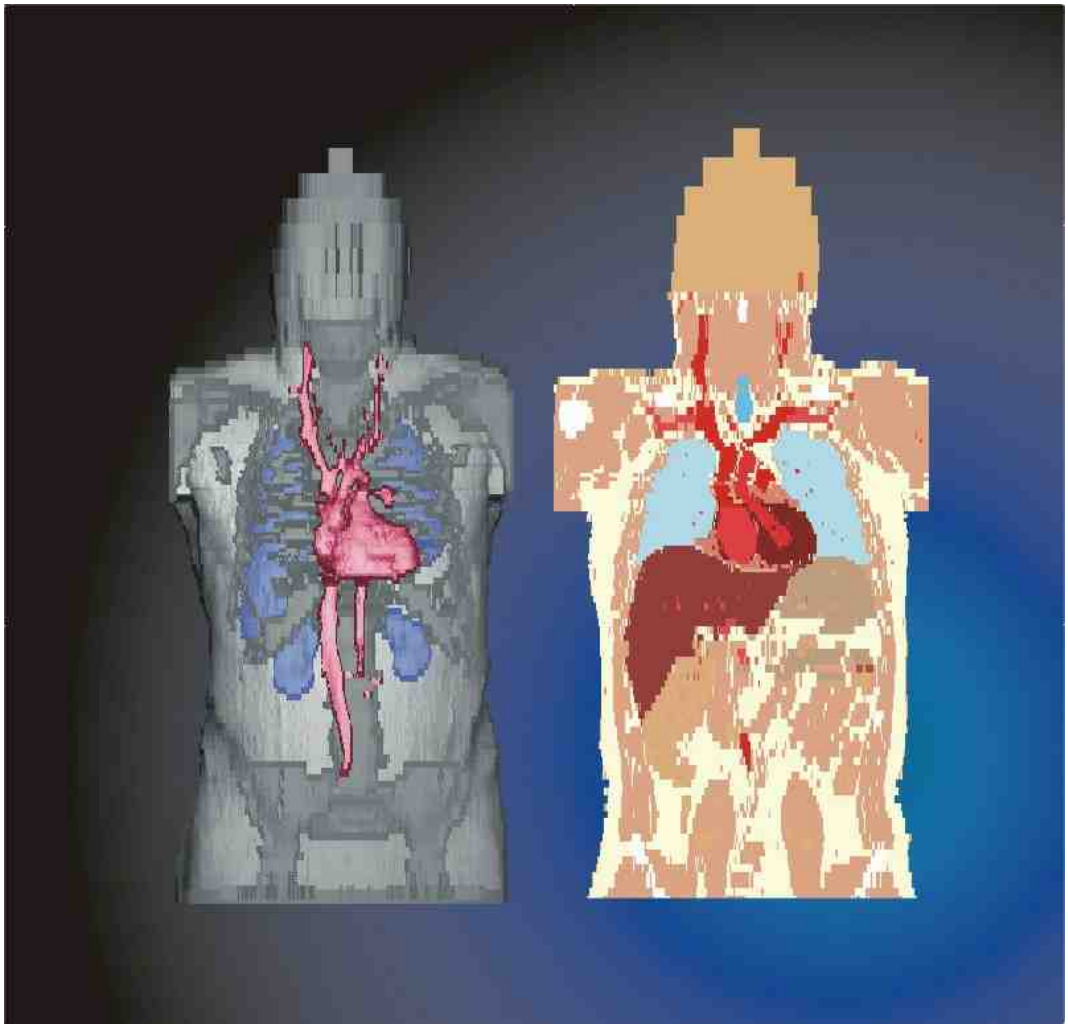

Figure 1. Outlook of the VHM model.

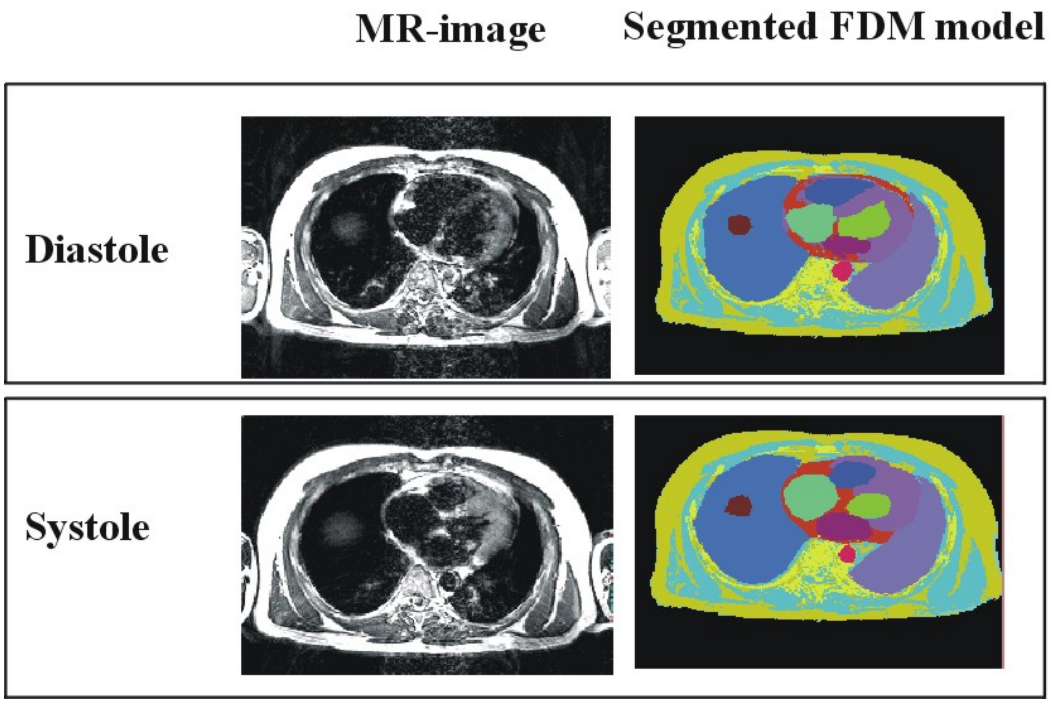

Figure 2. An example of the diastolic (top) and systolic (bottom) MR images and their segmented equivalents.

Study1: Effects of blood masses

For practical calculations the full accuracy of the VHM anatomical data has not yet been employed. A model was constructed using 4 mm and in lower thorax 8 mm intervals between slices. The model constructed comprised of 404 307 elements defined by a nonuniform rectangular grid. In the heart area the element size was 0.011 cm3 increasing to 0.7 cm3 on back of the thorax and further to 2.8 cm3 on lower section of the thorax. In this study four models from the VHM model with identical node structure but different inhomogeneities were employed:

- Case1: a model with full anatomical accuracy (the blood masses of intracardium, aorta, inferior and superior vena cava, pulmonary artery and vein and smaller vessels visible in the VHM data)
- Case2: a model without small blood vessels (other vessels and intracardiac blood masses were modelled)
- Case 3: a model without blood vessel (only intracardiac blood mass),
- Case 4: a model without blood masses

In each case the resistivity of those inhomogeneities not modelled was changed to 460 ohm cm representing an average sensitivity of the thorax.
The lead field of leads I and V3 was calcualted by reciprocal energization of the lead [8] (Figure 3). The effects of the inhomogeneities were assessed by calculating an average error vector length of the lead vector induced by the lack of inhomogeneities as shown in the equation as follows;

$$E_r(\%) = \frac{1}{n}\sum_{n}\frac{|(\vec{c}_n - \vec{c}'_n)|}{|\vec{c}_n|}\%$$

where cn and c´n are lead vectors obtained in a location n in the myocardium from a more accurate model and a model with reduced set of inhomogeneities, respectively.

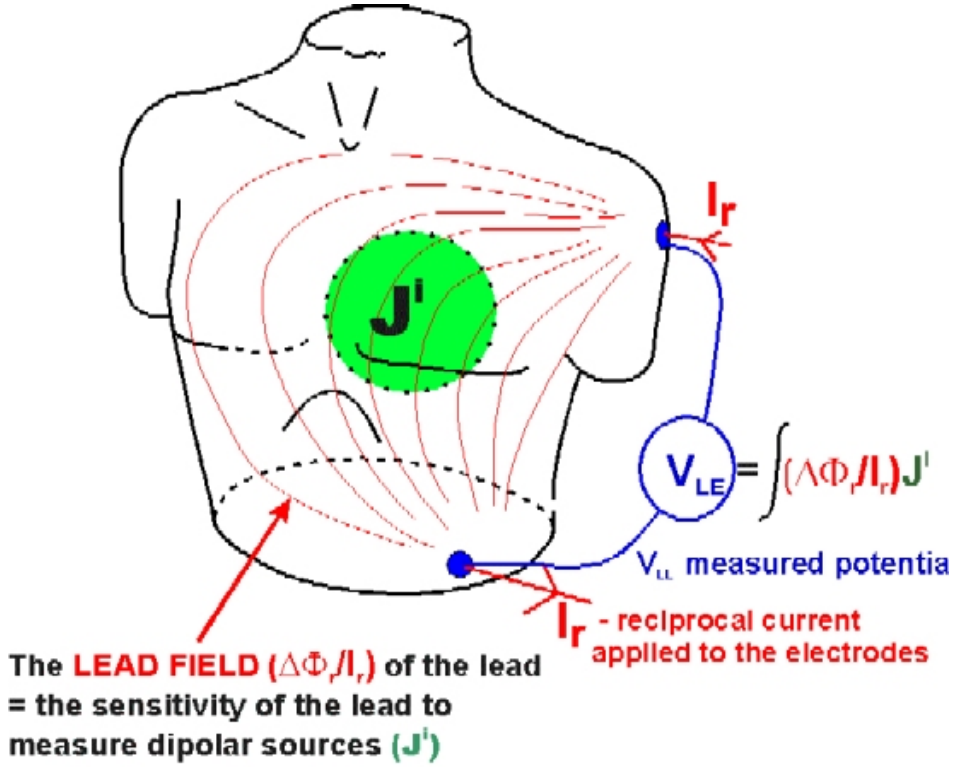

Figure 3. Calcualation of the lead field (sensitivity distribution) of an ECG lead to detect dipolar sources.

Effect of the variations in tissue conductivities

For this study computationally less demanding version of the VHM model with 83 987 elements was employed. The size of the elements varied from 0.3 cm3 in the heart region to 2.7 cm3 in the lower section of the thorax. Table 1 shows the conductivity values employed in the models. The effects of changes in the conductivity of various tissues were determined by increasing the conductivity of the tissues of the VHM model by 10%, a change that can be of physiological origin [2,3]. X, Y and Z components of a current dipole source located at the center of the heart were energized and body surface maps and corresponding body surface potential maps were calculated employing the FDM thorax model. The components are X: from back to front, Y: from left to right and Z: from feet to head [8]. The influence of the change in the conductivity value of heart muscle, skeletal muscle, all blood in the model, intracardiac blood, lungs, subcutaneous fat and heart fat were obtained by calculating the RMS difference on the body surface potentials between the original model and the model with altered conductivity.

Study 3: Effect of anatomical changes due to heart beat

The two models generatedfrom MR images gated at systole and diastole were employed. For practical calculations the full accuracy of the MR voxel data was not employed. A model was constructed using a nonuniform rectangular grid providing more accurate presentation of the anatomy in the heart area. The model constructed for this study comprised of 228163 elements. In the heart area the element size was 0.011 cm3 increasing to 0.68 cm3 on back of the thorax.The effect of the changes in the anatomy due to change of volumes of the inhomogeneities during the cardiac cycle was simulated by applying a current dipole source in four different locations of the cardiac muscle and calculating the resulting surface potentials. Dipole 1 was located in the septal area in the middle of the heart. Dipole 2 situated in the septal area but closer to the apex than dipole 1. Dipole 3 was applied in the vicinity of the lowest part of the apex, and dipole 4 located laterally in the left ventricle wall. The same coordinate points were used in both diastole and systole models. Then, the resulting surface potential distributions of both models were calculated.

To estimate the difference in forward problem an RMS error of the surface potentials was calculated between the models to assess the possible differences. In addition, a scaling factor was calculated to obtain an RMS error with a possible scaling of the potential removed.

To estimate the effect on inverse solution the locations of the dipoles were estimated based on an least square method based inverse algorithm that utilizes reciprocally calculated the lead fields [8,9,10]. The analyzed ECG lead arrangements include the standard 12-lead system and a 24-lead system. The effects of the anatomical changes were estimated by using the diastolic and systolic models for assessing the dipole location. In the reference case the inverse solution was based on the same model as the simulated source potential fields were calculated and in the test case the inverse problem was solved by using the potentials of the diastolic model in connection with the lead fields of the systolic model and vice versa. The absolute error of the spatial localization was obtained. Furthermore, in order to evaluate the modeling error generated by the cardiac cycle,

To have material to compare with, also the effect of electrode positioning accuracy on the localization procedure performance was estimated with the diastolic model by moving the electrodes on the surface of the body. Three types of electrode displacement were envisaged and simulated: transversal displacement of each electrode by 1.5 cm leftwards, longitudinal displacement by 2.0 cm downwards, and random displacement by either rightwards, leftwards or downwards by 1.5 cm, 1.5 cm, or 2.0 cm, respectively. The localization procedure was executed in all cases for both 12-lead and 24-lead systems and a total average localization accuracy in all dipoles in every orientation was calculated to evaluate the performance and the stability of the localization procedure. The results were compared with the localization results using the original electrode positions in the diastolic model.

Finally, the performance of the localization procedure was tested by interfering RMS noise to the potential values. The noise was generated at five levels ranging from 10% until up to 50% of the original values for both 12-lead and 24-lead system potentials of the diastolic model.

Results

Effect of blood masses

Table 3 indicates the mean error vector induced by the lack blood mass inhomogeneities for the lead fields of the leads I and V3. The intracardiac blood masses have the most profound effect as have been previously observed (case 4). The large vessels have more notable effect ranging 5 - 10% (case3). The small vessels have only minor effect (case2). The blood masses have larger effect on the properties of chest lead V3 than the standard lead I. Especially the intracardiac blood masses indicate this phenomenon, which is apparent the lead V3 having the measurement electrode close to the heart and the blood mass.

Table 3. *Effect of the blood masses on the lead vectors of the standard lead I and lead V3. Mean error vector and the standard deviation of the error vector induced by the lack of inhomogeneities.*

Model with all inhomogeneities: Blood volume: 610 ml, (Case 1)	Model without small blood vessels: Blood volume: 506 ml, (Case 2)		Model without blood vessels:Blood volume: 222 ml, (Case 3)		Model without blood masses: Blood volume: 0 ml, (Case 4)	
Error vector	*Compared to case 1*		*Compared to case 1*		*Compared to case 1*	
E_r(%), SD (%)	Lead I	Lead V3	Lead I	Lead V3	Lead I	Lead V3
Compared to case 1	E_r 1.3%, SD 3.0%	E_r 1.4% SD 3.7%	E_r 6.2 % SD 9.3 %	E_r 7.1% SD 7.8%	E_r 25.0% SD 14.1%	E 28.7% SD24.6%
Error vector	*Compared to case 1*		*Compared to case 2*		*Compared to case 3*	
E_r(%), SD(%) *Compared to the previous case*	Lead I	Lead V3	Lead I	Lead V3	Lead I	Lead V3
	E_r 1.3% SD 3.0%	E_r 1.4% SD 3.7%	E_r 5.6% SD 8.9%	E_r 7.2% SD 8.9%	E_r 24.3% SD 13.9%	Er 28.6% SD 24.4%

Effect of the variations in tissue conductivity

The change of ECG signal level generated by changing the tissue conductivity of all organs and that of the the intracardial blood masses are indicated in Figure 4 and full results in Table 4. The table shows the percentile changes in body surface potential levels of the X, Y and Z dipoles generated by 10% increase in the conductivity of each inhomogeneity.

Table 4 indicates that by increasing the conductivity of all organs by 10% increased the body surface potentials accordingly. On the other hand, the effects of the increased conductivity of the inhomogeneities were different. The increased conductivity of inhomogeneities close to

the heart dipole sources such as the blood masses and heart muscle increased the ECG potentials and the inhomogeneities close to the surface such as skeletal muscle and subcutaneous fat decreased the ECG signal. Conductivity values of the heart muscle and intracardiac blood masses had the largest effect. Conductivity change of the skeletal muscle had as well large influence. Changes in the conductivity of the low conducting lungs and subcutaneous fat had only small influence.

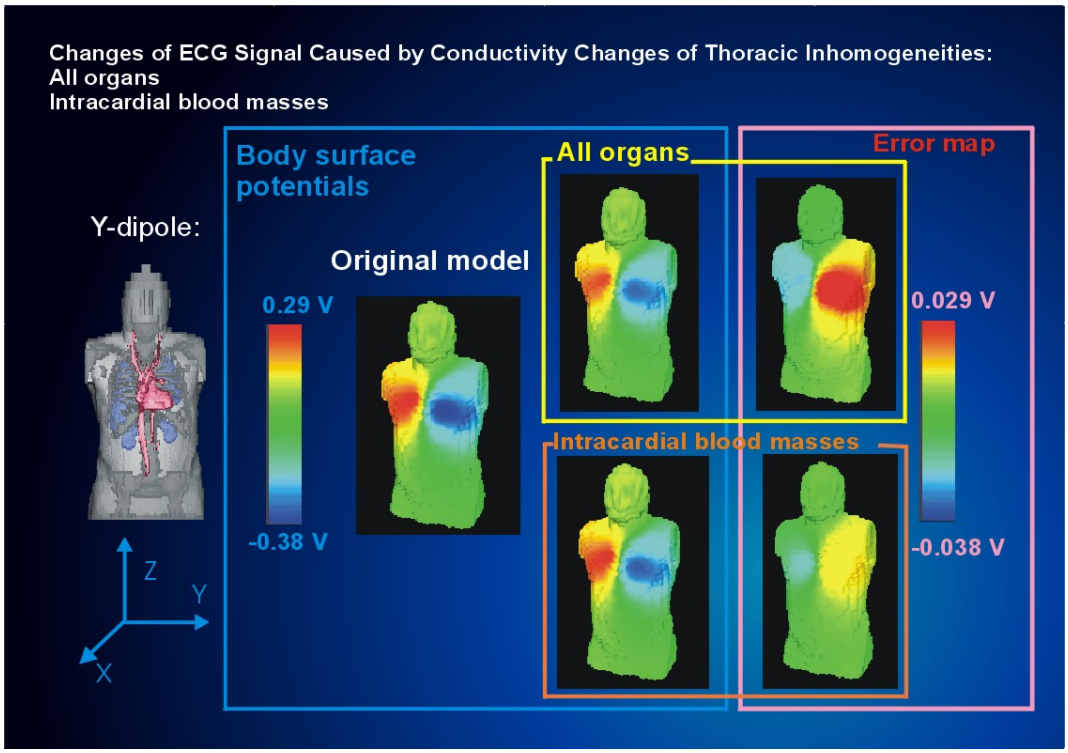

Figure 4. Body surface potential maps generated by a dipole at the center of the heart. Maps when the conductivity of all organs or the intracardial blood mass was increased by 10% and the error maps.

TABLE 4. *The changes in the body surface potentials of a dipole (%) caused by 10% increase in conductivity of various inhomogeneities*

	All organs	Heart Muscle	Skeletal muscle	Blood All	Intracardiac Blood	Lungs	Subcutaneous Fat	Heart Fat
X-dipole	10.8	10.4	-2.8	5.6	5.8	0.2	-1.1	0.2
Y-dipole	11.7	7.4	-4.9	8.8	9.7	1.9	-0.6	-0.1
Z-dipole	11.3	13.2	-4.1	3.0	2.2	-0.9	-0.4	0.1
|Average|	11.3	10.3	3.9	5.8	5.9	1.0	0.7	0.1

Effect of anatomical changes due to heart beat

Table 5 summarizes the average values of the surface potentials and their RMS errors between diastolic and systolic models in each dipole orientation. The mean values of the RMS errors of all dipoles in X, Y, and Z directions were 23.8%, 18.5%, and 20.1%, respectively. The mean RMS error values as scaling was removed reached 22.4%, 16.7%, and 8.9% in X, Y, and Z directions, respectively.

The average error values of the localization accuracy of all inverse problem solutions considered are summarized in Table 6. The average values are calculated including all four dipoles in all three orientations.

TABLE 5. *RMS error on body surface potential between diastolic and systolic models in each dipole orientation.*

Dipole	RMS error %	scaling factor	RMS error % scaling removed
1 -X	47.8%	1.05	43.9%
1 -Y	22.2%	0.87	26.1%
1 -Z	41.7%	1.22	20.2%
2 -X	11.3%	1.01	11.5%
2 -Y	25.3%	1.22	15.5%
2 -Z	12.6%	1.14	6.3%
3 -X	18.5%	0.86	15.6%
3 -Y	8.2%	1.04	7.0%
3 -Z	10.9%	1.07	4.9%
4 -X	17.7%	0.98	18.5%
4 -Y	18.4%	1.01	18.1%
4 -Z	15.1%	1.12	4.0%
Average	20.81%	1.05%	15.97%

TABLE 6. *The error of the inverse localization solutions in diastolic and systolic models (correct model) and the effects of modeling error (wrong systole or diastole model used), electrode displacement, and added RMS noise.*

Error type	Model and model modification	12 lead [mm]	24 lead [mm]
Diastolic model (correct model)	diastole potentials, diastole fields	11	7
Systolic model (correct model)	systole potentials, systole fields	15	7
Effect of the modeling error	diastole potentials, systole fields	14	15
	systole potentials, diastole fields	27	26
Effect of electrode displacement	transversal electrode displacement	18	14
	longitudinal electrode displacement	15	15
	random electrode displacement	13	18
Effect of added RMS noise	added random noise 10%	11	15
	added random noise 20%	11	14
	added random noise 30%	12	14
	added random noise 40%	13	13
	added random noise 50%	14	14

Conclusions

Study1: Effect of the blood masses

The strong effect of intracardiac blood masses manifested by our results has been observed in many studies. The other blood masses have not been generally modeled. Our results indicated that the effect of the large veins is as well important. Thus, these inhomogeneities should be modeled in order the get accurate forward solution for simulation studies and for the basis of the inverse solution. The smaller blood vessels had minor effect as could be expected. However, other errors such as uncertainty of the tissue conductivity values may mask the error generated by the lack the model of the large vessels, as indicated by our results (Table 4).

Study2: Effect of the changes in tissue conductivity

The conductivity values generally employed in thorax modeling are based on measurements done decades ago [6,7]. Furthermore, the measurements were done using tissue samples, which may not represent the true impedance of the living tissue. Thus there exits an uncertainty regarding the correct values of tissue conductivity. However, even more important contribution may emerge from the fact that tissue conductivity may change due to many physiological and pathological conditions such as posture changes and when electrolytic or water balance of the body is disturbed e.g., in diabetes or renal failure [2,3].
The 10% conductivity change is within the margins of body impedance change measured in dialysis patients [11]. Thus results here indicated that physiological changes of tissue conductivity produced marked changes in ECG signal levels.
These changes may cause variation in ECG parameters, which should be considered in ECG analysis. The influence of the blood hematocrit on the Brody effect of the intracardiac blood masses is well known [3] but marked changes in ECG have been observed that can not be explained by the Brody effect [12]. Thus our results indicate that some observed changes that are in partial contrast with the Body effect can be explained with conductivity changes in other compartments.
Furthermore, the results manifest the importance of the correct conductivity values to be used in thorax modeling. As shown in Table 4 especially critical is the conductivity of heart muscle and blood. According to our results the effect of 10% decrease in tissue conductivity was in the same order of magnitude as the influence of the great vessels. Thorax models can include many even minor anatomical details, thus the correct value of the tissue conductivity rises to a more relevant and critical problem than the accuracy and number of anatomical details in thorax models. Especially this is true in patient tailored models that should reflect the patient as an accurate volume conductor.

Study3: Effect of the anatomical changes due to heartbeat

A dipole source was applied to four different locations of the human thorax models constructed during end diastole and end systole. The results presented in Table 5 indicated that the error depended on the location and direction of the dipoles. Dipole 1 revealed largest errors. It was located at the septum demonstrating the effects of changing blood masses near the dipole in all directions. Other dipoles locating in the apex (2 and 3) and in the left ventricle wall (4) showed lower errors. Generally, the field of the Z dipole is only marginally affected by the changing anatomy, which is expected since the major anatomical changes take place near the ventricles mainly on the XY-plane.
It has been generally agreed that the data obtained from the 12-lead ECG system does not provide all the information regarding the electrical activity of the heart available on the body surface. The results of this study indicate that the overall localization accuracy improved in both diastolic and systolic models, reaching the level of 0.7 cm, respectively. Thus, it can be concluded that increasing the number of electrodes ameliorates the localization accuracy significantly even though the increase in number (from 12 to 24) is not particularly large.
Considering the diastolic-systolic and systolic-diastolic models reveals, however, the fact

that increasing the number of electrodes does not improve the localization accuracy if the model construction properties are inadequately chosen. Furthermore, it can be stated that an increase in the number of electrodes compensates neither the displacement of the electrodes nor the added RMS noise.
In conclusion, the results clearly indicate that the volumetric changes of the blood masses inside the heart must be taken into account for accurate modeling of the human thorax. In addition, this study revealed that the differences vary depending on the location of the dipole source. These aspects are especially important when considering the solution of the inverse problem before reliable clinical applications can be introduced.

Acknowledgments: This work has been kindly supported by The Ragnar Granit Foundation and The Wihuri Foundation.

References

[1] Klepfer, N., Johnson, C. and Macleod, R., "The effects of inhomogeneities and anisotropies on electrocardiographic fields - A 3-D Finite-Element study", IEEE Transactions on Biomedical Engineering, vol. 44, pp. 709-719, 1997.

[2] Kinoshita, O., Kimura, G., Kamakura, S., Haze, K., Kuramochi, M., Shimomura, K. and Omae, T., "Effects of hemodialysis on body surface maps in patients with chronic renal failure", Nephron, vol. 64, p. 580/586, 1993.

[3] Rosenthal, A., Restieaux, N. and Feig, S., "Influence of acute variations in hematocrit on the QRS complex of the frank electrocardiogram", Circulation, vol. XLIV, pp. 456-465, 1971.

[4] Kauppinen, P., Hyttinen, J. and Malmivuo, J., "A software implementation for detailed volume conductor modelling in electrophysiology using finite difference method", Computer Methods and Programs in Biomedicine, vol 58/2, pp. 191-203, 1998.

[5] Heinonen, T., Eskola, H., Laarne, P. and Malmivuo, J., "Segmentation of T1 MR scans for reconstruction of resistive head models", Computer Methods and Programs in Biomedicine, vol. 54, pp. 173-181, 1997.

[6] Rush, S., Abildskov, J. A. and McFee, R., "Resistivity of body tissues at low frequencies", Circulation, vol. 22, pp. 40-50, 1963.

[7] Geddes, L. A. and Baker, L. E., "The specific resistance of biological material - A compendium of data for the biomedical engineering and physiologist", Med. Biol. Eng., vol. 5, pp. 271-293, 1967.

[8] Malmivuo, J. and Plonsey, R., "Bioelectromagnetism. Principles and applications of bioelectric and biomagnetic fields", New York: Oxford University Press Inc., 1995.

[9] Dodel, S., "Statistische Methoden zur Lösung des Inversen Problems in der Elektrodynamik", University of Tübingen, Germany, 1996.

[10] Laarne, P., Kauppinen, P., Hyttinen, J., Malmivuo, J. and Eskola, H., "Effects of tissue resistivities on lead fields in head modelling", Medical & Biological Engineering & Computing, 1999;37:555-559.

[11] Tedner, B., Lins, L.-E., Asaba, H. and Wehle, B., "Evaluation of impedance technique for fluid/volume monitoring during hemodialysis", Int. J. Clin. Monit. Comput., vol. 2, pp. 3-8, 1985.

[12] Fuenmayor, A. J., Vasquez, C. J., Fuenmayor, A. M., Winterdaal, D.M. and Rodriquez, D., "Hemodialysis changes the QRS amplitude in electrocardiogram", International journal of cardiology, vol. 41, p. 141-145, 1993